This is the accepted version of:

The final publication is available at https://doi.org/10.2514/6.2022-2463

When citing this work, cite the original published paper.

Permanent link to this version
http://hdl.handle.net/11311/1196265

A decentralized approach for formation flying reconfiguration and maintenance using GNSS-based navigation

Francesca Scala* and Camilla Colombo†
Politecnico di Milano, 20156, Milano, Italy

Manuel Martin-Neira‡
European Space Agency, ESA-ESTEC, 2200 AG, Noordwijk, The Netherlands.

This paper presents the simulation results for the reconfiguration and maintenance of a novel three-satellites formation flying mission study. The analyses are based on a decentralized approach for the guidance, navigation, and control, to provide autonomous management of the formation flying by each satellite. The mission concept under analysis is developed in the remote-sensing field, to improve the performances of the Earth's observation missions for land and oceans applications and it is proposed as the new generation of ESA's SMOS mission. An in-house simulation suite, based on GNSS navigation, is used to assess the performances of the navigation and the control during nominal and nonnominal phases of the mission. The high-fidelity simulation analyses aim at assessing realistic performances of the proposed guidance and control strategies, based on low-thrust engine actuators. The work opens to the design of future formation flying missions in the Earth observation field, providing a baseline for the guidance, navigation, and control simulator.

I. Introduction

Tʜᴇ importance of distributed space systems for enhanced space mission was demonstrated for different applications, from technology demonstration to remote sensing missions, as described in [1–3]. This paper focuses on the latter scenario, exploiting the formation flying to enhance the potentials and the performances of future interferometry missions for Earth observation. Starting from the outcomes of ESA's Soil Moisture and Ocean Salinity (SMOS) mission in [4], a three-satellite formation flying mission concept with L-band aperture synthesis instruments (FFLAS) is considered in this paper, flying in the Low Earth Orbit (LEO) region. The mission concept has been presented in previous works [5], where a triangular formation is adopted to increase the spatial resolution of the observations up to 1 to 10 km, improving the current state-of-the-art resolution of 40 km of the SMOS mission, as in [1]. This paper presents the decentralized architecture and algorithms implemented for the guidance, navigation, and control (GNC) system for multiple satellites formation flying missions. It presents the simulation results for the main operational phase of the FFLAS mission study, focusing on the navigation and control accuracy achieved by the onboard algorithms. Different scenarios are considered to assess the performances, given the current capabilities of Global Navigation Satellites System (GNSS) receivers and vision-based sensors, and of the adaptive Extended Kalman Filter (EKF) for absolute and relative state reconstruction. The operational limitations introduced by the use of a low thrust control system are also included in the analysis, for a proper simulation of the possible uncertainties in the desired control.

The proposed GNC approach adopts a decentralized architecture for the autonomous management of the formation flying by each satellite of the formation, without the control by a reference spacecraft. For this reason, the platforms are assumed to have the same processing capabilities to handle the required computations by the GNC algorithm. Each satellite computes from the outputs of the onboard sensor the current state estimate of the whole formation with respect to the virtual central point. Then it transmits the information to the remaining satellites, via the onboard Inter-Satellite Link (ISL). From this information, each spacecraft can derive the current formation state and the orbital elements associated with a reference virtual spacecraft placed at the center of the formation. This approach aims at providing guidance, navigation, and control strategy that can be performed independently by each satellite of the formation, including the monitoring of the real-time risk of collision. The proposed analyses are based on the SKiLLeD simulation suite environment for multiple-satellites formation flying, developed at Politecnico di Milano in the MATLAB®/Simulink

---

*Ph.D. Student, Department of Aerospace Science and Technology, francesca1.scala@polimi.it.
†Associate Professor, Department of Aerospace Science and Technology, camilla.colombo@polimi.it.
‡Microwave Radiometer Engineer, European Space Agency, manuel.martin-neira@esa.int.

environment, based on C++ functions [6]. It allows high-fidelity simulations of the formation flying behavior during mission operations in an environment subject to orbital perturbations, such as the Earth's oblateness, atmospheric drag, and solar radiation pressure. The absolute dynamic of each satellite is propagated in the Earth Mean Equator and Equinox of the J2000 inertial reference frame. The relative dynamic is propagated in the framework of the Relative Orbital Elements, as well as considering the shape of the relative trajectory in the co-moving radial-transversal-normal orbital (RTN) frame.

The decentralized GNC approach is implemented for the FFLAS mission, assumed to fly in a 6 a.m. – 6 p.m. Sun-Synchronous Orbit at about 775 km of altitude. The main challenges of the formation reconfiguration and maintenance are given by the close proximity of the satellites during the scientific phase of the mission for Earth Observation. The three satellites of FFLAS will fly at the vertex of an equilateral triangular formation of 12 m sides. As a consequence, the assessment of control and navigation accuracy is of primary importance, and its precision level depends on several factors, such as the complexity of the system, the onboard algorithms, the hardware technology, etc. The analyses presented in this paper are based on state-of-the-art available technology for absolute and relative state reconstruction, such as the RUAG LEORIX GNSS receiver and the PRISMA vision-based sensors. Moreover, the use of the adaptive EKF to filter the sensor measurements can provide a navigation accuracy at centimeter level, as in [7]. A feedback linearization control algorithm is implemented to assess the control performances over the desired guidance reconfiguration and maintenance trajectories. The control of the formation is implemented with a low thrust engine, as required by the nominal formation baseline, which needs a continuous control profile to keep a rigid formation - with a fixed relative attitude profile - and safe flight conditions.

The manuscript is organized as follows. Section II presents a brief introduction of the FFLAS mission study, including the main performance and simulation requirements. Section III describes the Guidance, Navigation, and Control (GNC) simulator developed at Politecnico di Milano based on GNSS navigation sensors and high-fidelity dynamical description. Section IV presents the simulations and the results of the main test case scenarios. Moreover, it presents a discussion on the results and performance assessment for different operational phases of the FFLAS mission. Finally, Section V presents the conclusion of the manuscript.

II. FFLAS mission study

The analyses presented in this manuscript are developed for the FFLAS mission, but are valid for a general multiple satellite formation in LEO, based on GNSS navigation with a decentralized approach. The FFLAS mission wants to study the possibility to increase the virtual aperture of radiometer instruments with a formation of three satellites, flying at close distance in the range of 10 m. Some mission studies were already presented in the literature in this sense, as in [8, 9]. Following the work of [1], hexagonal array geometry is selected for the tree satellites, with a diameter of about 8 m. Moreover, the spacecraft will fly at the vertex of a triangular formation with dimension side in the order 10 m to 15 m. This configuration provides an equivalent aperture of 21 m for the L-band interferometers, achieving a spatial resolution of about 10 km, as described in [1, 4]. The increase in the spatial resolution performances with combined interferometry requires the satellites to fly in a fixed relative position during the scientific phase. Moreover, the payload requires a period of calibration once per month, to maintain the highest performances. This phase requires a maneuver for the formation to switch to an inertial orientation. This possibility was presented for the FFLAS case in [10], where optimal guidance based on low thrust technology was presented.

The nominal formation geometry for the interferometry phase is shown in Fig. 1. The satellites are placed at the vertex of an equilateral triangle, and the aperture plane lies in the transversal-normal (TN) plane facing the Earth direction, as shown in Fig. 1. The most important part of the study is the simulation for the verification of the possibility to achieve the following mission requirements:

- The relative position between the phase centers of any pair of antenna elements, belonging to the same array or different arrays, shall be controlled to be within ± 2 cm (1 σ) from the nominal values (nominal hexagonal grid underlying the 3 arrays).
- The real-time relative position between the phase centers of any pair of antenna elements, belonging to the same array or different arrays, shall be known to ± 2 cm (1 σ).
- The ground reconstruction of the relative position between the phase centers of any pair of antenna elements, belonging to the same array or different arrays, shall be known within ± 2 mm (1 σ).

For this purpose, a GNC simulator with a high-fidelity dynamical propagator is proposed to evaluate the performances for the two main operational phases of the mission study, the Earth pointing phase and the payload calibration phase.
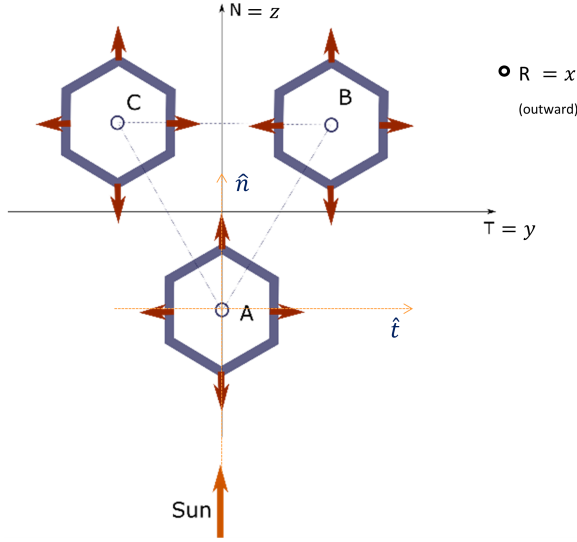
Fig. 1   FFLAS nominal geometry in Earth pointing configuration.

1. Reference frames definition

This section presents the main reference frames currently used in the GNC simulator design. Concerning the absolute reference frame, we consider the classical Earth-centered Equatorial Coordinate System (EME2000) for the high-fidelity dynamical propagation of each satellite. The dynamical propagation of the absolute state of the satellites is performed in EME2000, to include the major sources of perturbation of the LEO region. Then the True-of-Date (ToD) reference frame is introduced in the simulator, to include the effects of nutation and precession in the dynamical propagation. It is related to the current epoch, and, for this reason, the axes of the coordinates system are time-dependent. The values in ToD are computed from the dynamical propagation in EME2000, to gain the knowledge of the nutation and precession effects and are used to compute the relative motion in RTN and ROEs. Consequently, we define the local Hill orbital frame (RTN) with the following vector triad, to describe the relative motion of two or more satellites with respect to the reference orbit:

- The x-axis of the RTN frame is aligned with radial direction of the reference orbit: $e_x = \mathbf{r}/r$
- The z-axis is aligned with the angular momentum of the reference orbit: $e_z = \frac{\mathbf{r} \times \mathbf{v}}{|\mathbf{r} \times \mathbf{v}|}$
- The y-axis completes the right-hand side frame: $e_y = e_z \times e_x$

Moreover, we also considered the ROEs framework to describe the orbital elements of each satellite in the formation (deputies) with respect to the reference orbital elements (chief). This final representation allows a semi-analytical description of the dynamical model, with a deep insight into the relative motion, and the definition of the inter-satellite collision avoidance constraint in terms of the eccentricity-inclination vector separation. The reference orbit for the FFLAS is the virtual central point of the triangular formation. We selected the reference orbit equal to the nominal one of the SMOS mission, i.e. a 6 a.m. to 6 p.m. Sun-Synchronous orbit at 775 km of altitude.

III. Guidance, Navigation, and Control system design

This section presents the GNC simulator developed to evaluate the performances of the operational scenarios of the FFLAS study. This tool aims at assessing the performances of the system and at supporting functional and performance tests for feasibility studies. The main outcome is the accuracy in the control and in the navigation solution reconstruction that is achievable on-board. A key aspect is the possibility to perform an autonomous GNC during the nominal phase of the mission, without the need of including continuously the ground reconstruction in the algorithms. This will support the feasibility of performing the main operatiional modes independently, including the collision risk assessment and the eventual transition to a safe mode. For this purpose, a control in the centimeters level is required for a safe flight of the spacecraft, which nominally, are just 10 meters apart. The requirement in the control is correlated to the onboard navigation solution, which is required to be lower than the control solution. So far, several missions demonstrated the feasibility of a precise millimeter and centimeter relative navigation in LEO, for the ground and

onboard reconstruction, respectively, as discussed in [11]. Global Navigation Satellite System (GNSS) based navigation systems were implemented on several occasions, thanks to the possibility to recover information on both the absolute and relative state of the satellites, such as for the on-ground navigation system of the GRACE mission. For LEO satellites, the first challenge in the design of navigation algorithms is related to the presence of uncertainties in the carrier phase measurements and to the limited duration time of the continuous positioning signal from one single GNSS satellite. These conditions require proper algorithms and onboard filter development, to provide a precise relative navigation reconstruction onboard the satellites. The possibility to implement a combination of GNSS and vision-based navigation could also be considered to increase the accuracy and the reliability in the position reconstruction [12]. Additional optical sensors could provide accurate measurements of the inter-satellite distance, to be combined by the navigation filter with the GNSS information.

A. High-fidelity dynamical propagator

The in-house high-fidelity dynamical propagator, called Simulation Kit for Logic Layout Design of Formation Flying (SKiLLeD) developed by Gaias [13], was adapted to the FFLAS environment in preparation for the performance simulations. The simulator aims at providing support to the design of relative GNC algorithms for LEO missions. The absolute orbits of a chief and a deputy satellites are propagated in the EME2000 and then a conversion between osculating/mean elements is provided after the transformation into the TOD reference system. The main propagation is based on a C++ algorithm which includes the main gravitational perturbations effects due to the gravitational $J_{m,n}$ terms. For propagating the FFLAS formation, we introduced some modification to the original code, as follow:

- Inclusion of the possibility to simulate simultaneously one chief satellite and up to N deputies' satellites, by vectorizing the C++ based functions.
- Development of a high-fidelity atmospheric drag model in the perturbing acceleration of the relative motion, in a separated C++ function, based on the NRLMSISE-00 model of [14].

The high-fidelity propagator is made of three main blocks. The first is the Orbit Dynamics Block, based on C++ S-function for the MATLAB®/Simulink environment. It takes as input parameters the absolute EME2000 state of the reference and of the satellites in the formation. It computes the accelerations of an Earth-orbiting satellite under the influence of the Earth's harmonic gravity field a_{grav}, the atmospheric drag a_{drag}, and the commanded thrust from the GNC simulator a_{cmd}. The acceleration is computed in the EME2000 Orbital frame from the information on the position and velocity of a generic satellite at time t:

$$a_{s/c}(t) = a_{grav}(t) + a_{drag}(t) + a_{cmd}(t) \tag{1}$$

The acceleration due to the harmonic gravity field is computed from the information on the position of the satellite at time t and the n_{max}, m_{max} parameters, which represents the zonal and harmonic order of the gravitational field. The geopotential gravity field implemented in the model is based on the GRACE Earth Gravity model 02 (GGM02S), as in [15]. This model is based on the analysis of the in-flight data collected by GRACE during 363 days of measurements. It describes the gravitational field up to 160×160 degree order and includes the gravity anomalies over the surface of the Earth.

The second block is the State Conversion Block from EME2000 to the ToD reference frame. The transformation is based on the rotation matrix $R_{eme2tod}$, from [16]:

$$\mathbf{X}_{ToD} = \mathbf{R}_{eme2tod}\mathbf{X}_{EME} \tag{2}$$

Where $R_eme2tod$ includes both the effect of nutation and precession. Finally, the third block is the State Conversion Block for the computations of relative quantities. It implements several S-function blocks for the computation of the relative state of the deputies:

- The relative cartesian block implements the conversion from the inertial state (position and velocity) of two spacecraft to the Cartesian relative state (position and velocity), in the local Hill orbital frame of the chief satellite. It is implemented in a C++ function, taking as input the chief and the deputy inertial state.
- The ROE Block implements the conversion from the Keplerian elements of the chief and deputy satellites to the relative orbital element framework. It is implemented in a C++ function, taking as input the Keplerian elements of chief and deputies' satellites

B. Guidance algorithms

The guidance algorithm is based on a convex optimization problem, which aims at providing the delta-v optimal trajectory solution. Given different case scenarios for the FFLAS, the guidance trajectory is computed together with the reference control law. As fully described in [10], the optimal trajectory problem is written in a convex formulation to guarantee a unique solution. Moreover, the problem is defined to include the main constraint for the FFLAS satellites, such as the maximum thrust level for the control law, the desired final configuration or the maintenance period, and the minimum distance among the satellites to guarantee a safe formation. The latter is important to avoid possible nonnominal flight conditions, which could result in a collision among the satellites. The optimization procedure is based on the MATLAB® environment, and it is inserted in the closed-loop GNC simulation, for the definition of the reference trajectory and control. These are the inputs for the control block, described in Section III.E The schematics for the guidance block is shown in Fig. 2.
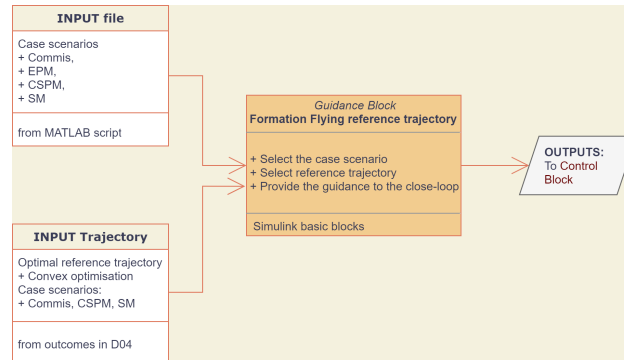

Fig. 2   Block diagram schematics of the Guidance algorithm.

C. Decentralized architecture

The proposed GNC analysis aims at verifying the main operational phases and the GNC performances of FFLAS. A decentralized approach is selected for autonomous GNC management without the mediation from a specific satellite. Each spacecraft is supposed to have the same computational and data-handling capabilities and to autonomously elaborate their GNC algorithms. The continuous mutual exchange of GNSS navigation data enables the reconstruction of the absolute formation status at each time instant onboard each satellite. Moreover, each spacecraft could recover, from the information on the absolute formation status, its relative state associated with a virtual spacecraft at the center of the formation triangle. The elements of the virtual satellite are propagated in time thanks to the onboard dynamical propagator. The GNC algorithms are elaborated by each satellite of the formation in the RTN reference frame of the virtual platform. This architecture is shown in Fig. 3, where the virtual platform is identified by dashed contours, and the FFLAS satellites are called "A", "B", and "C" respectively. During the nominal phases of the mission, it is important the correct sharing of data among the satellites, to enable the autonomous navigation and path planning of the formation. The navigation logic for the exchange of data is selected as follow:

- Each satellite (A, B, or C) transmits the current state to the remaining satellites.
- Each satellite receives the data from the other platforms.
- Each satellite computes the current navigation state estimate in the local frame of the virtual satellite.

D. Navigation algorithms and sensor design

The Navigation block includes the procedures and algorithms necessary to estimate the absolute and the relative state of the satellites in the formation. For the FFLAS formation, we consider a decentralized architecture, where the reference satellite computes the absolute state measurement and shares the information with the other satellites in the formation. At this point, each vehicle computes its relative state through a navigation filter. Specifically, the onboard sensors provide measurements on the position and velocity evolution of each satellite during the time. These measurements are subject to noise and disturbances, caused by the sensor's accuracy on the measures, and the navigation algorithms aim at filtering and processing such information, to generate a good estimation of the actual state of the satellite. The navigation algorithm is made of two main blocks. The first is the GNSS receiver block, which provides
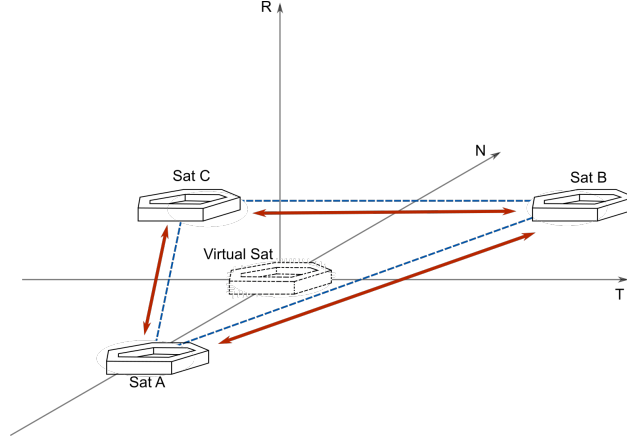
Fig. 3   Selected logic for the navigation system based on a decentralised approach.

the measure absolute and relative state from the ground truth reference for the satellites in the formation. Then the absolute state estimation block and the relative state estimation block consist of an Extended Kalman Filter (EKF), which is used for absolute state and relative state reconstruction from the measurements values.

1. GNSS receiver block

The GNSS receivers can provide three different measures: the pseudo-range ρ_{pr}, the carrier phase ρ_{cp}, and the doppler measurement $\dot{\phi}$. The former is the range between the GNSS satellite and the user, in our case one of the satellites of the formation. It is subject to some noises, the receiver clock error, the ionospheric error, and other sources. The second instead, measure the difference between the carrier phase of the GNSS and the receiver satellite, and the doppler measurement provides information on the range rate [17]. In this simulator, information on the absolute position and velocity given by the GNSS receiver is obtained by perturbing the state of the satellites in ToD with a noise term. The high-fidelity propagation in ToD from the SKiLLeD environment is considered representative of the ground truth dynamics of the formation, whereas the noise term is representative of the sources of uncertainties in the signal received from the GNSS satellites. A zero-mean Gaussian noise used to perturb the ground truth propagation is selected according to the physical properties of the GNSS receivers for FFLAS.

2. Absolute and relative state estimation block

The state estimation block is based on an EKF, which processes the information from the GNSS satellites and the state variable connected to the other satellites in the formation. The inputs to the state estimation block are the satellite state computed from the GNSS sensors and the formation status. The latter is exchanged among the formation with the inter-satellite communication link. The initial covariance on the satellite state knowledge is given as a covariance matrix P_0. Moreover, an additive measurement noise with covariance R_0 is included in the model, as well as a measurement function to recover the state from the nonlinear dynamics. In the estimation filter, the knowledge on the onboard nonlinear dynamical propagator for the absolute state reference is the state transition value and it implements the main LEO perturbing effects. The algorithm includes both the mean J_2 contribution of the Earth's oblateness and the drag effects. Besides, to improve the performances of the state reconstruction, the Jacobian function of the dynamical propagator is included in the model. Finally, the process noise is included in the state transition value with the covariance matrix Q_0, which represents the additive process noise. The parameters used in the simulator to provide the absolute and the relative state estimation in the close-loop of the GNC simulator are used as input for the (EKF) to estimate the actual state from the GNSS sensor measurements. The variance of the position and velocity is selected according to the estimated error in the measurements to make the filter converge to the ideal trajectory:

- For the absolute estimation, an error in the measurements in the order of 1 m and 0.002 m/s, for the position and velocity respectively, is considered in the variance definition.
- For the relative navigation estimation, an error in the measurements in the order of 1 cm and 0.001 mm/s is considered for the position and velocity, respectively.

For both absolute and relative state estimation, the initial state estimation covariance matrix P_0 is selected for the

initial step and then at each time is updated in the algorithm considering the residual error from the previous step. Consequently, an adaptive EKF is considered in the navigation block, to improve the state reconstruction performances.

Relative navigation   The relative state is computed from the GNSS measurements between a couple of satellites in the formation. Between two receivers of two different satellites, i and j, the single difference carrier phase measurement can be computed as:

$$\rho_{sdcp}^{ij}(t) = \rho_{cp}^{j} - \rho_{cp}^{i} \tag{3}$$

This procedure can be applied to any couple of satellites in the formation. Similarly, a single difference among the doppler measurement can be computed to provide the range-rate change in time:

$$\Delta\phi^{ij} = \phi^{j} - \phi^{i} \tag{4}$$

The advantage of using the differential measurement is the canceling of the ionospheric noise, which affects the accuracy of the GNSS measurements. Moreover, it provides a value with smaller uncertainties and external noises. Now the state vector for the formation can be computed at each time instant as:

$$x_{REL} = x_{ABS}^{i}, \quad x_{REL}^{1i}, \quad ..., \quad x_{REL}^{ji}, \quad ..., \quad x_{REL}^{(N-1)i} \tag{5}$$

Where the index i stands for the reference satellite in the formation and the index j represents the other satellites for $j = 1 : N - 1$, with N the number of vehicles in the formation. The relative state x_{REL} represents the position and velocity of satellite j with respect to satellite i. In this work, we start from the absolute state estimation in the ToD frame, and we recover the relative state of the satellite j of the formation with respect to the reference i satellite. The measurement vector is the relative state of the satellites in the formation corrupted by a zero-mean Gaussian noise, as in [6]. The relative navigation filter is used to estimate the relative position and velocities of the satellites in the formation from the noisy measurement.

Navigation error   The characterization of the estimation error is important to assess the performance of the navigation filter. The state estimation error can be computed at each time step by subtracting the actual $x(t_k)$ and the estimated state $\hat{x}(t_k)$:

$$e_{NAV}(t_k) = x(t_k) - \hat{x}(t_k) \tag{6}$$

Another parameter to assess the performance of the state estimation is the standard deviation, from the filter covariance matrix P_k:

$$\sigma_k = \sqrt{P_k} \tag{7}$$

Both the navigation error and the standard deviation provide a performance of the navigation solution with respect to the actual state at each time instant.

E. Control algorithms and actuators design

The Control Block includes the procedures and algorithms necessary to provide a commanded thrust to the satellites in the formation. It takes both the information on the desired state from the Guidance Block and the estimated state from the Navigation Block. The control algorithm is composed of two main blocks. The controller block provides the ideal control to the close-loop simulator from the error difference between the desired and the estimated satellites state. Then the actuator block implements the ideal control in the onboard thrusters, considering the technological limitations to provide the actual control to the close loop simulator. For the FFLAS formation, we consider a low thrust architecture, with the engines lying on the x_b, z_b plane of the body frame of each satellite. Specifically, the QinetiQ T5 engines are considered in the analysis. The control algorithm requires two input information. First, the desired relative xRTN or ROEs state of the deputies, given by the Guidance block, and second the estimated absolute and relative states of the deputies, given by the Navigation block.

1. Control block

The control algorithm implements the maneuver commanded by the guidance algorithms and provides the command control to the actuators. It implements an optimal control to minimize the error between the actual state and the desired state, from the navigation reconstruction and the guidance algorithms, respectively. The Controller Block implements a feedback control law for nonlinear system dynamics and in particular a feedback linearization of the system error. The following procedure is implemented:

- The system error is computed from the comparison between the desired and the estimated relative states of the Deputies: $e(t) = x_{RTN}(t) - x_{d_{RTN}}(t)$
- Positive-definite control gain parameters ($k_1 and k_2$) are introduced to compute the equivalent input for ideal control definition.
- The onboard dynamics (J_2 and drag) is considered the reference for the Deputies evolution.

From the equivalent input and the reference dynamic of the Deputies, the ideal control is computed. Finally, the ideal control in the RTN frame is provided as input to the Actuator Block.

2. Low thrust actuator model

For an accurate simulation of the formation performances, we characterize the actual control that the onboard thruster can provide. The FFLAS satellites are equipped with four low-thrust engines, the QinetiQ T5, which are oriented in the x,z plane of the body frame. The implemented procedure can be applied also to different low-thrust engines. The maximum thrust is limited by a saturation value, to guarantee that the required thrust is below the technological limit. Moreover, a control delay term is introduced to represent a real actuator, which will always introduce a delay in the ideal control. This is mainly due to the intrinsic time delay in the actuator response. Consequently, the ideal control is elaborated and transmitted by the propulsion control unit to the engine assembly, which has an intrinsic delay in the response time. Finally, noise terms and error terms are introduced on the thrust level, to account for the real behavior of the engine, as well as to simulate errors in the attitude of the satellites. For the FFLAS case, the QinetiQ T5 performances are the following:
- Thrust range: 0 to 25 mN
- Thrust error: 5% for thrust level <3 mN and 1% for thrust level > 3 mN
- Thrust noise: 1.2 mN/$\sqrt{\text{Hz}}$ at 1 mHz and 0.012 mN/$\sqrt{\text{Hz}}$ at 100 Hz

IV. Simulation Results

This section describes the results of the simulations for formation flying maintenance of the FFLAS mission study. This paper focuses on the preliminary results of the GNC simulator for the formation maintenance during the scientific mode, for Earth observation purposes, and the formation transition to the calibration phase.

A. Simulation settings

This section describes the settings used for the simulation scenario. The simulations are based on MATLAB®/Simulink R2021a, operating on an Intel Core i7-7700, 3.60 GHz processor. The simulation time is about four orbital periods, for a preliminary evaluation of the GNC performances. This period is enough to introduce the nonlinearity of the relative dynamics and to analyze the convergence of the controller and the navigation filter. We considered the gravity field due to the gravitation harmonics up to a 6x6 order, and the influence of drag during the motion. The time step was selected equal to 1.0 s to provide the velocity vector as the rate of change of the position vector in 1-second. For the navigation system, the performance of the RUAG Leorix GNSS receiver is considered in the simulation. The initial states of the FFLAS satellites are reported in Table 1, where the relative position is expressed in the RTN frame for each satellite with respect to the central virtual point of the triangular formation. The formation geometry of the science mode is shown in Fig. 4 (left), where A, B, and C represent the satellite of the formation and O is the central virtual point. The initial conditions in the RTN frame are computed from the representation in the inertial ToD frame, which also considers the effect of nutation and precession.

B. Science and calibration phase definition

The science and the calibration phase are the two main operational phases of the FFLAS formation during the nominal scenario. During the science phase, the satellites are in a triangular formation with the aperture plane of the payloads pointing to the Earth. During this phase, the three satellites fly in formation, according to the nominal formation geometry, shown in Fig. 4 (left). The ISL for data exchange is represented by the red, green, and blue rectangles, whereas the solar panels are Sun pointing, represented by the orange line. By system requirement in [5], the ISL antennas shall remain in the same relative configuration during different mission phases. Once per month, the interferometers require a calibration period, when their aperture plane should point toward the zenith. During this phase, the satellites should be able to change their attitude of the aperture plane, from nadir to inertial pointing. As described

in [10], to maintain the correct data link among the satellites, an attitude maneuver is not enough for this purpose, but the formation needs to make a reconfiguration to switch the position of satellites B and C, as in Fig 4 (right). The idea of the analysis is to evaluate the compliance of the simulator with the required accuracy level of both the navigation and the controller. The configuration conditions for the calibration geometries are reported in Table 2.
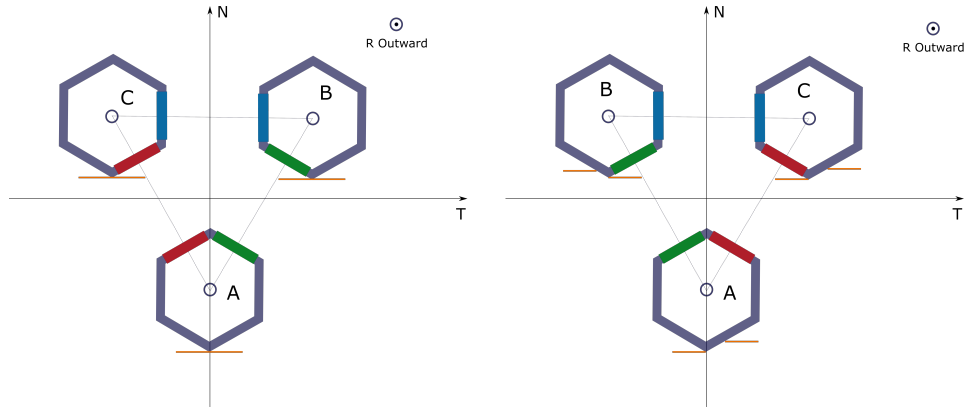

Fig. 4   FFLAS nominal configuration during the science (left) and the calibration (right) phases.

C. Simulations results

The simulation aims to provide the performances of formation maintenance and maneuver during the payload calibration scientific phase of the mission. During the simulation, the closed-loop control algorithm relies on onboards GNSS navigation for reconstructing the state of the formation. Moreover, the ground state reconstruction is evaluated to assess the feasible accuracy level, and the control algorithm provides a command thrust to the onboard actuators, which are limited to 25 mN of maximum thrust. Finally, the onboard actuators provide the thrust only in the x-z body axis, corresponding to the transversal and normal direction of the RTN frame.

The ideal trajectory followed during the transition to and back the calibration configuration is shown in Fig. 5. This

Table 1   Simulation settings for the initial conditions of the FFLAS case.

Guidance	Values
Reference SSO	$\{7.1531 \cdot 10^6 \, \text{m}, \, 6.4 \cdot 10^{-4}, \, 2.114 \, \text{rad}, \, 3.434 \, \text{rad}, \, 3.36 \, \text{rad}\}$
Sat A	$\{-1.9 \cdot 10^{-3}, \, 6.5 \cdot 10^{-3}, \, -5.369, \, 0, \, 0, \, 0\}$
Sat B	$\{-1.9 \cdot 10^{-3}, \, 6.236, 5.369, \, 0, \, 0, \, 0\}$ m, m/s
Sat C	$\{-1.9 \cdot 10^{-3}, \, -6.236, 5.369, \, 0, \, 0, \, 0\}$ m, m/s
Navigation	Values
Absolute position error	1.0 m 3D rms
Absolute velocity error	2 mm/s 3D rms
Carrier phase error	< 1.8 mm rms
Code measurement error	< 0.7 mm rms

Table 2   Simulation settings for the calibration case.

Guidance	Values
Sat A	$\{-1.9 \cdot 10^{-3}, \, 6.5 \cdot 10^{-3}, \, -5.369, \, 0, \, 0, \, 0\}$
Sat B	$\{-1.9 \cdot 10^{-3}, \, -6.236, 5.369, \, 0, \, 0, \, 0\}$ m, m/s
Sat C	$\{-1.9 \cdot 10^{-3}, \, 6.236, 5.369, \, 0, \, 0, \, 0\}$ m, m/s

trajectory was studied in [10], considering a convex formulation of the problem to assess the delta-v optimal maneuver. It can be seen that satellites B and C follow a specular trajectory for the transition, while satellite A has to remain stable in its original position. The trajectories of the satellites are identified with three different colors, while the central point represents the reference virtual trajectory. Fig. 5 (right) represents the time evolution of the position and velocity in the RTN frame. The simulations steps are the following:

1) One orbital period in Earth pointing configuration is simulated, for formation maintenance during the science phase.
2) The maneuver from Earth to zenith pointing is simulated, where satellites B and C switch their position.
3) Then, an attitude maneuver is performed to point the satellites' payload toward the cold sky.
4) Once the calibration configuration is reached, the inertial pointing is maintained for about 30 minutes, implementing formation maintenance.
5) At the end of the calibration phase, another attitude maneuver is performed, to point the payload again to toward the Earth and a formation maneuver is simulated to return to the original science phase configuration.

The necessity to include an optical link to improve the real-time and post-processing navigation accuracy will be evaluated.
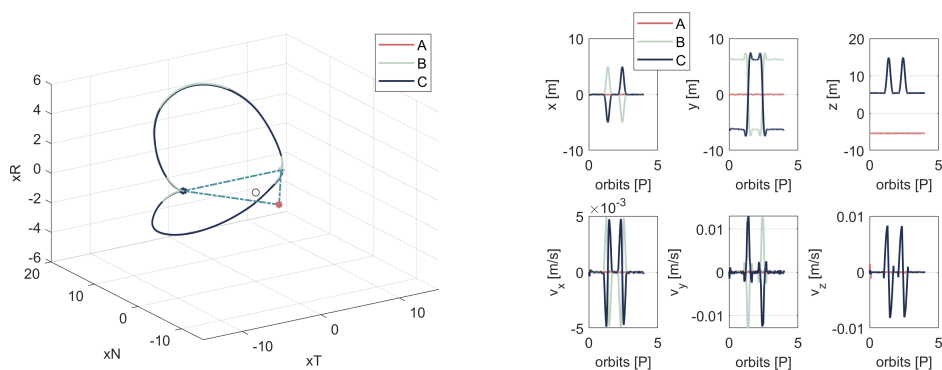

Fig. 5   FFLAS nominal reconfiguration trajectory during the transition between science and calibration phases. three dimensional representation on the left, and time evolution of the RTN components on the right.

1. Control profile

The control thrust profile required during the calibration phase is shown in Fig. 6, where the control in the body frame is on the left, while the one in the EME2000 frame is on the right. It can be seen that the control required for satellite A consists of the pure formation maintenance control, with a constant thrust in the normal (x_b) direction of about 10 mN. On the other hand, satellites B and C start with the formation maintenance control before entering the maneuver control profile to pass to the calibration configuration. The thrust to switch their position is only in the normal and transversal direction (x_b, z_b). Around the second orbital period, there is a 30-minute slot where the satellites maintain the zenith pointing for the calibration of the payload thanks to the maintenance control profile. The maximum thrust is limited by the technological performances of the QinetiQ T5 engine of 25 mN maximum, as represented by the red line in the body-fixed frame control in Fig. 6.

2. Navigation accuracy

An important parameter to consider in the performance evaluation of the simulation is navigation accuracy. The simulation is performed considering GNSS-based navigation onboard the satellites, while the possible optical/vision-based sensor could be included to improve the reliability of the results. The solution from the onboard navigation state reconstruction is important to guarantee the autonomous GNC setting for FFLAS during the payload calibration phase of the mission. The estimation of the state is used as an input to the control block to define the commanded thrust to the actuator. Thanks to the implementation of the EKF onboard the satellite, the real-time onboard navigation accuracy remains in the order of 1 to 2 cm. The navigation solution for each satellite in the formation is shown in Fig. 7, where the shadowed part is the confidence interval of the navigation solution.
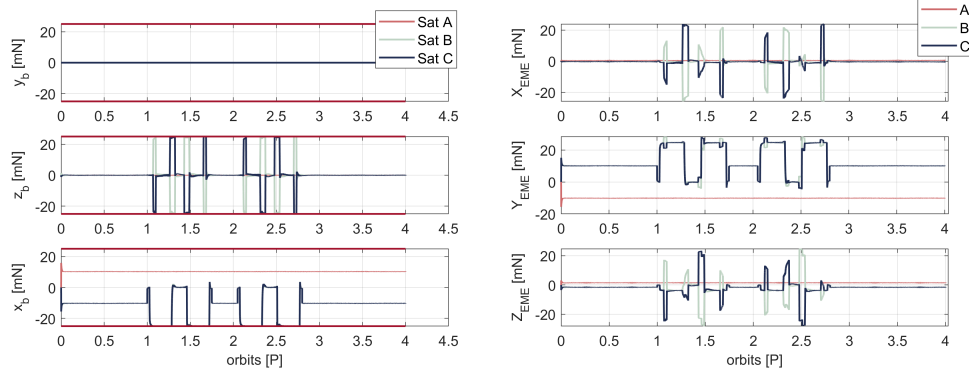
Fig. 6 Control thrust for the maneuver to and back the Cold Sky Pointing Mode phase in the body-fixed frame (left) and in the Earth Mean Equatorial Frame (right). The red line represents the maximum available thrust from the QinetiQ T5 (25 mN).
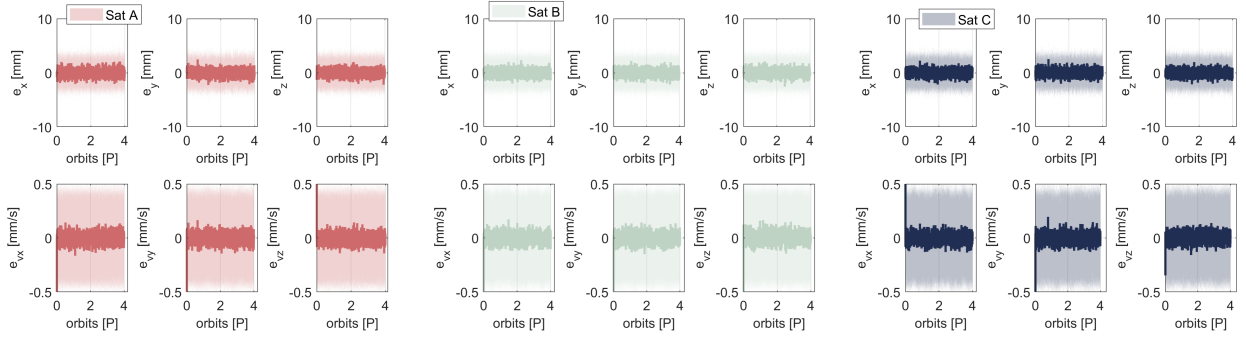

Fig. 7 Onboard navigation accuracy for the three satellites A (left), B (center), C (right), during the transition to and back the calibration phase, in the RTN frame.

3. Accuracy of the formation control

A Linear Quadratic Regulator (LQR) control is implemented to follow the optimal trajectory for the initial reconfiguration. The control matrix in the RTN frame, where we assumed that the desired attitude is guaranteed by the onboard actuators. The satellites provide control only in the transversal and normal directions. The LQR weights are selected after a trade-off parametric analysis to improve the control outcome. The weights for the matrix Q and R are chosen as:

$$Q = \begin{bmatrix} 10 & 0 & 0 & 0 & 0 & 0 \\ 0 & 0.9 & 0 & 0 & 0 & 0 \\ 0 & 0 & 10 & 0 & 0 & 0 \\ 0 & 0 & 0 & 1e5 & 0 & 0 \\ 0 & 0 & 0 & 0 & 1e5 & 0 \\ 0 & 0 & 0 & 0 & 0 & 1e5 \end{bmatrix} \tag{8}$$

$$R = \begin{bmatrix} 10 & 0 & 0 \\ 0 & 5 & 0 \\ 0 & 0 & 1 \end{bmatrix} \cdot 10^8 \tag{9}$$

Starting from these weights matrices, the controller performance is computed via the difference between the guidance trajectory and the actual trajectory. the former is the delta-v optimal strategy for the formation reconfiguration to the calibration scenario. The following assumptions have been made during the simulation:

- the state reconstruction is based only on the onboard navigation, to allow an autonomous formation reconfiguration even when the ground station is not in view.

- the control could improve significantly including in the closed-loop the ground reconstruction information for the state of the satellites.

Fig. 8 shows the error in the control for the calibration transition phase. After the initial instants where the controller needs to converge, the error in the control is limited in the range 1 to 10 cm, over the desired position of the satellites, with some local peak of about 20 cm accuracy. Particularly, in the initial and final time, the formation maintenance in Earth pointing configuration is implemented, with a control accuracy for the relative position in the order of a few centimeters (1 to 10 cm). In the central part, some peaks around 20 cm of accuracy can be identified at the moment when begins the maneuver to switch positions between satellites B and C. This is due to the need for the controller to converge again for a different situation than the formation maintenance for science configuration. In a successive phase of the mission (phase B), an optimization of the controller is envisioned, to improve the controller performances in both the formation maintenance and maneuver implementation. Moreover, the possibility to include the ground in the closed-loop navigation will improve significantly the performances, reducing the navigation error in the order of a few millimeters.
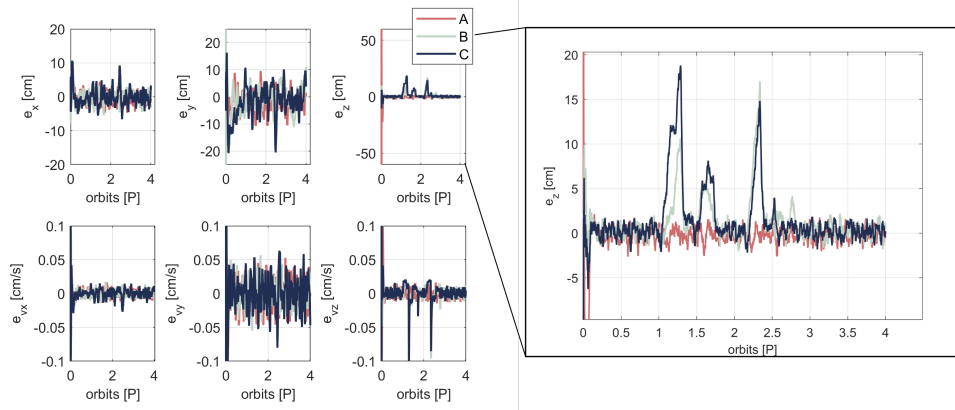

Fig. 8   Error in the formation control, for the three satellites, in the RTN frame. The error on the z is zoomed to better represent the order of magnitude of the error after the convergence of the algorithm.

V. Conclusions

This paper provides a simulator of guidance, navigation and control for multiple-satellite formation flying. It relies on a high-fidelity dynamical propagator, based on a C++ environment, and provide a baseline for the controller and the navigation filter to be included in the closed-loop dynamics. The scenario considered the FFLAS formation on a quasi-circular SSO orbit in the LEO environment. Consequently, the main perturbing effects have been considered in the dynamical propagator, such as the Earth's oblateness and the drag effect, while the solar radiation pressure and the third body perturbations are included in the propagation noise. The relative navigation problem based on the GNSS sensor is presented, for the estimation of the relative position and velocity states. A preliminary result of the performances of the EKF is discussed for the analysis case, providing the navigation error in the relative state reconstruction of each satellite in the formation. However, the performances of the EKF strongly depends on the selected onboard dynamic and the sensor performances (noise and covariance). For this reason, accurate analysis on the robustness of the filter will be performed as part of the study for the FFLAS mission design. Moreover, the design approach for the controller is presented, based on feedback linearization error. Other approaches could be considered for more accurate control of the system dynamics, which could better include the nonlinearities and uncertainties in the system. To conclude, the proposed analysis provides a baseline procedure for assessing the GNC performances of a multiple satellite formation flying mission, based on the GNSS navigation system. The high-fidelity simulations aim at assessing realistic performances of the proposed guidance and control strategies. The navigation and control accuracy for the FFLAS mission are expected to be in the centimeters order, to comply with the mission requirements, and to provide safe mission operations. The automatic transition to the calibration phase is presented, providing a baseline approach for onboard operations. The methodology applies to other multi-satellite missions in similar orbital scenarios, also considering the recent trend of employing low-thrust engines onboard scientific satellites.

References

[1] Martín-Neira, M., Suess, M., Karafolas, N., Piironen, P., Deborgies, F., Catalán, A., Vilaseca, R., Montero, J., Puertolas, M., Outumuro, D., Corbella, I., Durán, I., Duffo, N., Materni, R., Mengual, T., Piqueras, M. A., Olea, A., Solana, A., Closa, J., Zurita, A., Ramírez, J. I., Breinbjerg, O., Bjørstorp, J. M., Kaslis, K., Kristensen, S. S., Oliva, R., Onrubia, R., Camps, A., and Querol, J., "Technology Developments for an Advanced L-Band Radiometer Mission," *IGARSS 2020 - 2020 IEEE International Geoscience and Remote Sensing Symposium*, 2020, pp. 6507–6510. https://doi.org/10.1109/IGARSS39084.2020.9324378.

[2] Scipal, K., and Davidson, M., "The SAOCOM-CS mission: ESA's first bistatic and tomographic L-band mission," *2017 IEEE International Geoscience and Remote Sensing Symposium (IGARSS)*, 2017, pp. 123–124. https://doi.org/10.1109/IGARSS.2017.8126909.

[3] Roscoe, C. W., Westphal, J. J., and Mosleh, E., "Overview and GNC design of the CubeSat Proximity Operations Demonstration (CPOD) mission," *Acta Astronautica*, Vol. 153, 2018, pp. 410–421. https://doi.org/https://doi.org/10.1016/j.actaastro.2018.03.033, URL https://www.sciencedirect.com/science/article/pii/S0094576517314042.

[4] Zurita, A. M., Corbella, I., Martín-Neira, M., Plaza, M. A., Torres, F., and Benito, F. J., "Towards a SMOS Operational Mission: SMOSOps-Hexagonal," *IEEE Journal of Selected Topics in Applied Earth Observations and Remote Sensing*, Vol. 6, No. 3, 2013, pp. 1769–1780. https://doi.org/10.1109/JSTARS.2013.2265600.

[5] Scala, F., Gaias, G., Colombo, C., and Martìn-Neira, M., "Formation Flying L-Band Aperture Synthesis: Design Challenges and Innovative Formation Architecture Concept," *71st International Astronautical Congress (IAC 2020)*, Vol. IAC-20-C1, The CyberSpace Edition, 2020, pp. 1–10. URL http://hdl.handle.net/11311/1153224.

[6] Scala, F., Colombo, C., Gaias, G. V. M., and Martin-Neira, M., "GNSS-based Navigation for a Remote Sensing Three-Satellite Formation Flying," *SpaceOps 2021 Virtual Edition*, Vol. SpaceOps-2020,7,x1482, Cape Town, South Africa, 2021, pp. 1–18. URL http://hdl.handle.net/11311/1172794.

[7] Leung, S., and Montenbruck, O., "Real-Time Navigation of Formation-Flying Spacecraft Using Global-Positioning-System Measurements," *Journal of Guidance, Control, and Dynamics*, Vol. 28, No. 2, 2005, pp. 226–235. https://doi.org/10.2514/1.7474, URL https://doi.org/10.2514/1.7474.

[8] Krieger, G., Moreira, A., Fiedler, H., Hajnsek, I., Werner, M., Younis, M., and Zink, M., "TanDEM-X: A satellite formation for high-resolution SAR interferometry," *IEEE Transactions on Geoscience and Remote Sensing*, Vol. 45, No. 11, 2007, pp. 3317–3341. https://doi.org/10.1109/TGRS.2007.900693.

[9] Moreira, A., Krieger, G., Hajnsek, I., Papathanassiou, K., Younis, M., Lopez-Dekker, P., Huber, S., Villano, M., Pardini, M., Eineder, M., et al., "Tandem-L: A highly innovative bistatic SAR mission for global observation of dynamic processes on the Earth's surface," *IEEE Geoscience and Remote Sensing Magazine*, Vol. 3, No. 2, 2015, pp. 8–23. https://doi.org/10.1109/MGRS.2015.2437353.

[10] Scala, F., Gaias, G., Colombo, C. C., and Martín-Neira, M., "Design of optimal low-thrust manoeuvres for remote sensing multi-satellite formation flying in low Earth orbit," *Advances in Space Research*, Vol. 68, No. 11, 2021, pp. 4359–4378. https://doi.org/https://doi.org/10.1016/j.asr.2021.09.030, URL https://www.sciencedirect.com/science/article/pii/S0273117721007456.

[11] Di Mauro, G., Lawn, M., and Bevilacqua, R., "Survey on guidance navigation and control requirements for spacecraft formation-flying missions," *Journal of Guidance, Control, and Dynamics*, Vol. 41, No. 3, 2018, pp. 581–602. https://doi.org/10.2514/1.G002868.

[12] Gaias, G., Ardaens, J.-S., D'Amico, S., et al., "The autonomous vision approach navigation and target identification (AVANTI) experiment: objectives and design," *9th International ESA Conference on Guidance, Navigation & Control Systems, Porto, Portugal*, 2014.

[13] Gaias, G., Colombo, C., and Lara, M., "Analytical Framework for Precise Relative Motion in Low Earth Orbits," *Journal of Guidance, Control, and Dynamics*, Vol. 43, No. 5, 2020, pp. 915–927. https://doi.org/10.2514/1.G004716.

[14] Picone, J., Hedin, A., Drob, D. P., and Aikin, A., "NRLMSISE-00 empirical model of the atmosphere: Statistical comparisons and scientific issues," *Journal of Geophysical Research: Space Physics*, Vol. 107, No. A12, 2002, pp. SIA–15.

[15] Tapley, B., Ries, J., Bettadpur, S., Chambers, D., Cheng, M., Condi, F., Gunter, B., Kang, Z., Nagel, P., Pastor, R., et al., "GGM02–An improved Earth gravity field model from GRACE," *Journal of Geodesy*, Vol. 79, No. 8, 2005, pp. 467–478. https://doi.org/10.1007/s00190-005-0480-z.

[16] Montenbruck, O., and Gill, E., *Satellite orbits: models, methods and applications*, Springer Science & Business Media, 2012.

[17] "Hardware-in-the-loop simulations of GPS-based navigation and control for satellite formation flying," *Advances in Space Research*, Vol. 46, No. 11, 2010, pp. 1451–1465. https://doi.org/https://doi.org/10.1016/j.asr.2010.08.012, URL https://www.sciencedirect.com/science/article/pii/S0273117710005260.